Supplementary Material (ESI) for Journal of Materials Chemistry

Supporting information

Magnetically Separable Porous Graphitic Carbon with Large Surface Area as Excellent Adsorbents for Metal Ions and Dye

*Li Sun, Chungui Tian, Lei Wang, Jinlong Zou, Guang Mu, Honggang Fu**

Key Laboratory of Functional Inorganic Material Chemistry, Ministry of Education of the People's Republic of China, Heilongjiang University, Harbin 150080 P. R. China Fax: (+86) 451 8666 1259; Tel: (+86)451 8660 9115 E-mail: fuhg@vip.sina.com.

1. TEM images

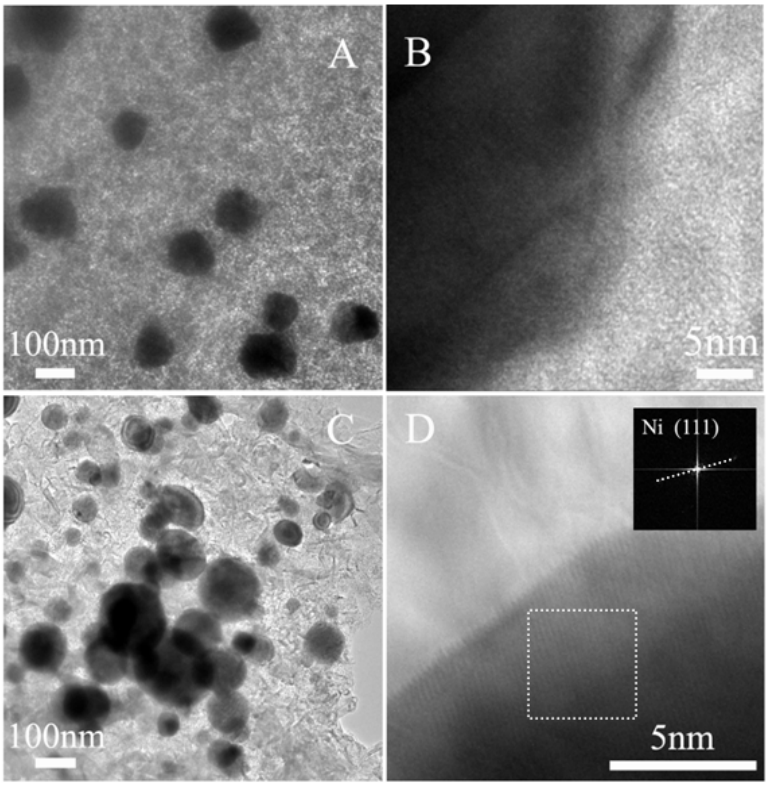

Fig. S1 TEM images (A) and HRTEM images (B) of the MPGC-800 sample; TEM micrographs (C) and HRTEM image (D) of the MPGC-1000 sample; Inset in (D) shows the two-dimensional Fourier transforms of the selected area at the surface of magnetic nickel particles.

2. Brunauer–Emmett–Teller (BET) surface areas

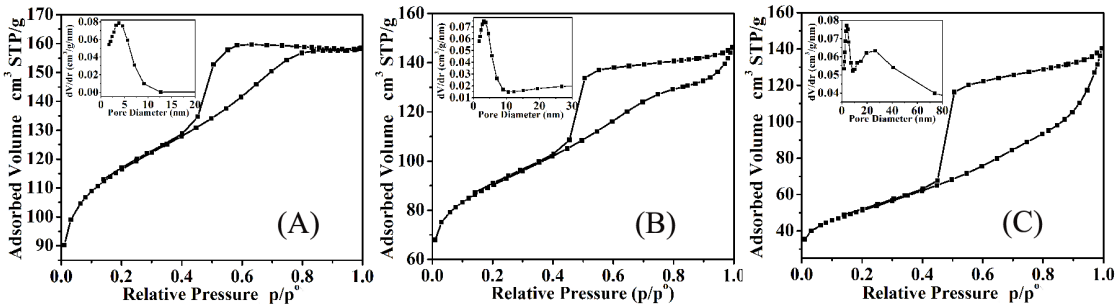

Fig. S2 Nitrogen adsorption/desorption isotherm and pore size distribution (inset) of NSC-800 (A), NSC-900 (B) and NSC-1000 (C), respectively.

3. Magnetic Properties

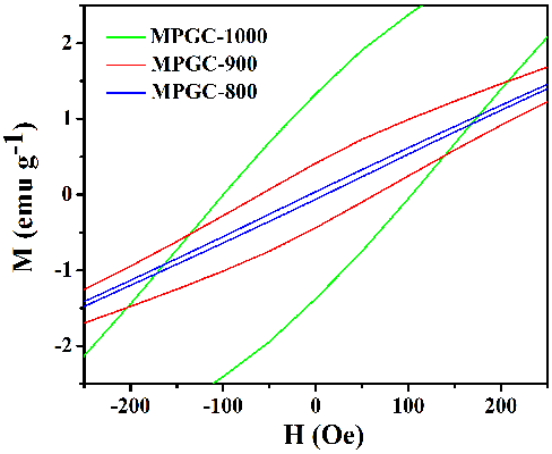

Fig. S3 Field-dependent magnetization curve measured at 300 K under larger magnification for the MPGC-based materials

Table. S1 Magnetic properties of the MPGC-based materials

Samples	M_S (emu g^{-1})	M_R (emu g^{-1})	normalized M_S (emu g^{-1})	M_R/M_S	H_c (Oe)
MPGC-800	6.3	0.04	21.8	0.006	7.06
MPGC-900	6.1	0.41	21.6	0.067	61.44
MPGC-1000	8.9	1.35	31.8	0.152	100.79

4. Kinetic studies

The first-order rate equation is given as:

$$\log(q_e - q_t) = \log q_e - \frac{k_1}{2.303} t \qquad \text{(S1)}$$

The pseudo-second-order equation is given as:

$$\frac{t}{q_t} = \frac{1}{k_2 q_e^2} + \frac{t}{q_e} \qquad \text{(S2)}$$

Where q_e and q_t are the dye and metal ions amounts adsorbed on the adsorbents (mg g^{-1}) at equilibrium and at time t, respectively; k_1 and k_2 is the rate constants of first and second order adsorptions, in min^{-1} and g mg^{-1} min^{-1}. In fact, it is required that calculated equilibrium adsorption capacity values, q_e (cal.), should be in accordance with the experimental q_e (exp.) values.

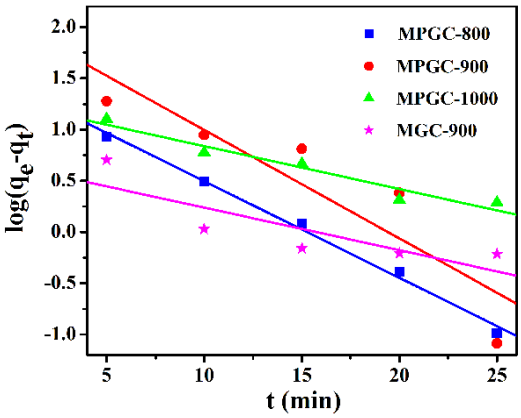

Fig. S4 The pseudo-first order sorption kinetics of RhB onto MPGC and MGC materials.

Table. S2 Kinetic parameters for adsorption of RhB on the MPGC and MGC-900 materials

Samples	q_e(exp.)	Pseudo-first-order			Pseudo-second-order		
	(mg g^{-1})	q_e(cal.) (mg g^{-1})	k_1 (min^{-1})	R^2	q_e(cal.) (mg g^{-1})	k_2(g mg^{-1} min^{-1})	R^2
MPGC-800	67.9	27.4739	0.2171	0.9973	68.7285	0.0346	0.999
MPGC-900	73.0	112.9536	0.2437	0.9042	75.3012	0.0108	0.997
MPGC-1000	60.5	18.0306	0.0963	0.9719	61.1247	0.0182	0.998
MGC-900	37.7	4.4884	0.0954	0.8416	37.8800	0.0704	0.999

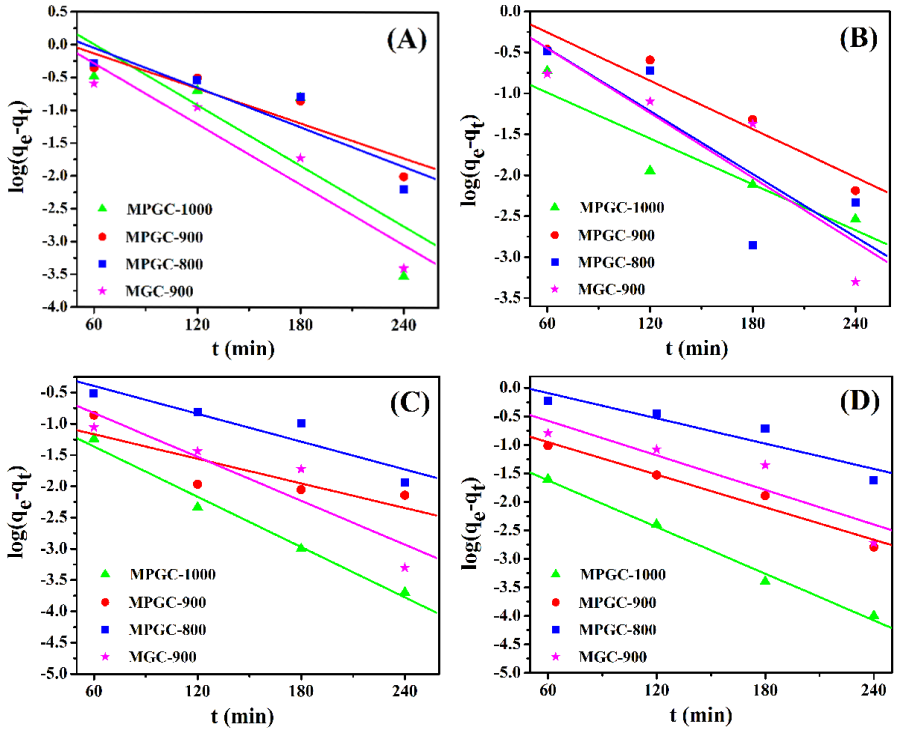

Fig. S5 The pseudo-first order sorption kinetics of metal ions Cd^{2+} (A), Cu^{2+} (B), Ag^{+} (C), and Au^{3+} (D) onto MPGC and MGC-900 materials

Table. S3 Kinetic parameters for adsorption of metal ions on the MPGC and MGC-900 materials

sample	Metal ions	q_e (exp.)(mgg^{-1})	Pseudo-first-order			Pseudo-second-order		
			q_e(cal.)(mgg^{-1})	k_1(min^{-1})	R^2	q_e(cal.)(mgg^{-1})	k_2(mgg^{-1}min^{-1})	R^2
MPGC-1000	Cd^{2+}	3.80	8.4275	0.3535	0.8277	3.8292	0.0577	0.9994
	Cu^{2+}	3.56	0.3697	0.0215	0.9302	3.5793	0.0561	0.9999
	Ag^{+}	3.71	0.2758	0.0308	0.9922	3.7169	0.6733	1
	Au^{3+}	3.94	0.1568	0.02326	0.9816	3.9455	0.1443	0.9999
MPGC-900	Cd^{2+}	3.67	2.4832	0.0203	0.9163	3.7224	0.0411	0.9991
	Cu^{2+}	3.54	2.1572	0.0226	0.9605	3.5834	0.0563	0.9995
	Ag^{+}	3.71	0.1688	0.0151	0.8446	3.7205	0.2726	0.9999
	Au^{3+}	3.92	0.4146	0.0219	0.9815	3.9317	0.3006	0.9999
MPGC-800	Cd^{2+}	3.26	3.5431	0.0230	0.9061	3.3234	0.0368	0.9987
	Cu^{2+}	3.23	2.0910	0.0295	0.8462	3.2724	0.0697	0.9995
	Ag^{+}	3.57	1.1222	0.0171	0.9342	3.5988	0.0705	0.9997
	Au^{3+}	3.89	2.2436	0.0170	0.9384	3.9500	0.0324	0.9988
MGC-900	Cd^{2+}	1.59	4.3084	0.3528	0.9509	1.6283	0.08917	0.9991
	Cu^{2+}	1.64	2.1818	0.0303	0.8943	1.6612	0.1297	0.9996
	Ag^{+}	2.37	0.7484	0.0269	0.9188	2.3835	0.2867	0.9999
	Au^{3+}	1.87	1.0659	0.02326	0.9158	1.8895^{+}	0.1353	0.9997

5. The existing state of absorbed metal ions in MPGC samples

For precious metal ions of Au^{3+} and Ag^{+}, the sample before and after adsorption of Au^{3+} and Ag^{+} were analyzed by XPS method, and the results are displayed in **Fig. S6**. As shown in **Fig. S6A**, the XPS survey spectrum for fresh MPGC-900 adsorbent exhibits a broad C1s peak that consists of three contributions: graphite (284.2– 284.9 eV), phenols, ethers or alcohols (285.4–286.3 eV), carbonyls (287.2–287.9 eV). The MPGC-900 material after adsorption Au^{3+} ions are characterized by XPS spectra as shown as **Fig**. **S6C**. The peaks at 84.1 eV and 87.8 eV are the characterization of Au4f. The results indicated that the adsorbed gold ions in adsorbent existed in the zero valence state. We also studied the existing state of silver ions in adsorbent. However, it is hard to distinguish the peaks between Ag^{+} and zero valence Ag from XPS spectra (**Fig. S6E**). For the purpose of confirmation the existing state of silver ions in adsorbent, the spent MPGC materials were characterized by X-ray diffraction (XRD) profile as shown as **Fig. S6F**. A typical reflection pattern of silver demonstrated that the absorbed Ag^{+} metal ions in adsorbents existed in the zero valence state, which is similar to the above analytic results of gold. As shown in **Fig. S6B and Fig. S6D,** we can see that the carboxyl and carbonyl peaks decreased after Au^{3+} and Ag^{+} adsorption compared with **Fig. S6A**, suggested that the functional groups on the MPGC-900

surface participation in the redox reaction of Au^{3+} and Ag^{+} transform to elemental silver and elemental gold, respectively. This mechanism has been reported by the previous study that the functional groups on the carbon surface, such as carboxyl and carbonyl, could be reduce Au^{3+} and Ag^{+} ions to zero valence gold and silver. (The corresponding reference has been referred as **Ref. 30** in the manuscript)

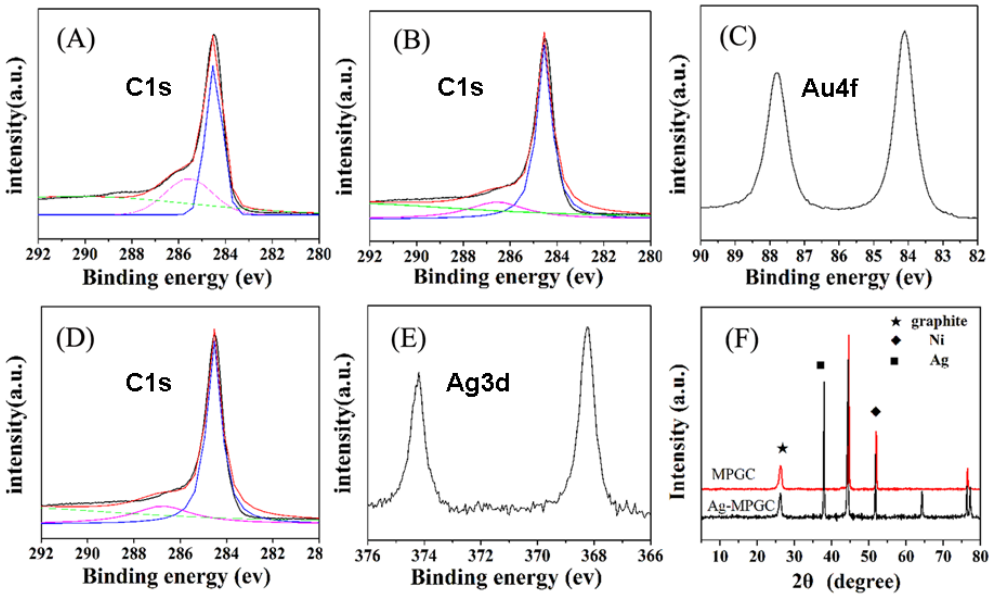

Fig. S6 XPS spectra of the (A) fresh MPGC-900 adsorbent C1s, (B) and (C) are the C1s and Au4f of the MPGC-900 after adsorption Au^{3+} ions, (D) and (E) are the C1s and Ag3d of the MPGC-900 after adsorption Ag^{+} ions, respectively. (F) is the XRD pattern of the MPGC-900 after adsorption Ag^{+} ions.

In order to research the existing state of heavy metal ions, the adsorbent after adsorption Cd^{2+} and Cu^{2+} ions were also performed by XPS. The Cd3d and Cu2p spectra displayed in **Fig. S7**. As shown in **Fig. S7A**, the peak of $Cd3d_{5/2}$ belongs to the characterization of Cd^{2+}. The satellite peak in $Cu2p_{3/2}$ at 943.7 eV indicates the existent of Cu^{2+} (**Fig. S7B**). Consequently, unlike precious metal ions (gold and silver), heavy metal ions of cadmium and copper exist as the state of $Cd^{2+}$and Cu^{2+} in adsorbent.

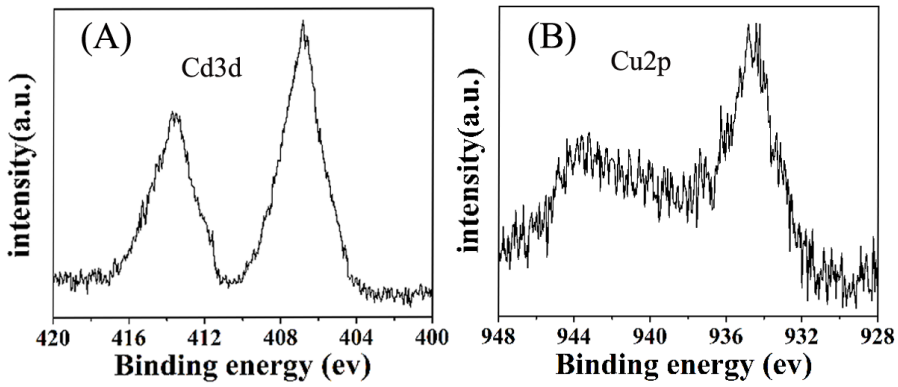

Fig. S7 X-ray photoelectron spectra of spent MPGC-900 adsorbent (A)Cd3d and (B)Cu2p.

In summary, MPGC materials are promising in the field of efficient separation for heavy metal ions and noble ions from aqueous solutions.

6. The effect of pH on the magnetic response of the MPGC-900 material

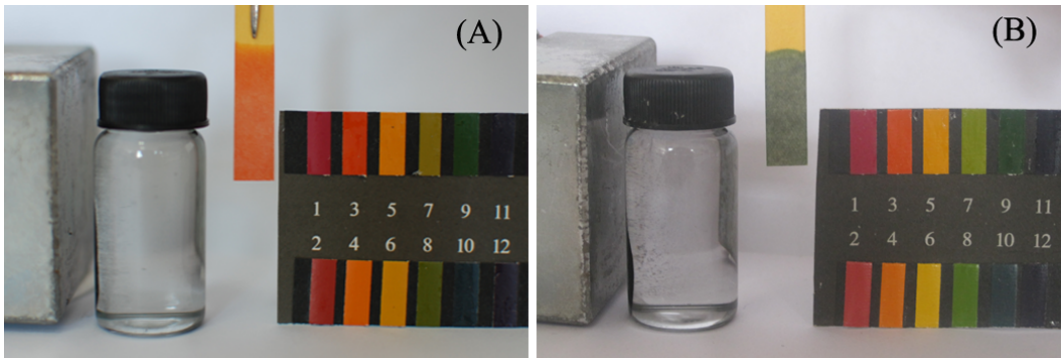

Fig. S8 Photo of magnetic response of MPGC-900 in acidic solution of pH (3 ~ 4) (A) and in alkaline solution of pH (8 ~ 9) (B) after 5 days' stewing.